Inhibition of Sulphuric Acid Corrosion of Mild Steel by Surfactant and Its Adsorption and Kinetic Characteristics

Prathibha B.S[1], P. Kotteeswaran[2], V. Bheemaraju[3]

[1]Department of chemistry, BNM Institute of Technology, Bengaluru-70, India
[2] Department of chemistry, RAMCO Institute of Technology, North Venganallur Village, Krishnapuram Panchayat, Rajapalayam Tamil Nadu- 626 117, India
[3] Department of chemistry, Dr. Ambedkar Institute of Technology, Bengaluru, India

Abstract: The corrosion inhibition effect of surfactant, N,N-Dimethyl-N-(2-Phenoxyethyl)dodecan-1-aminiumbromide(DPDAB) on mild steel corrosion in 0.5M Sulphuric acid was investigated by weight loss, potentiodynamic polarization and Electrochemical impedance spectroscopic techniques. DPDAB is an excellent inhibitor and its inhibition efficiency increases with increase in concentration and maximum inhibition efficiency was observed above the critical micelle concentration (CMC). The polarization curves reveal that DPDAB acts as mixed type inhibitor with predominantly of anodic type. The corrosion inhibition efficiency of DPDAB increases with increase in concentration and decreases with increase in temperature from 298K to 308K and then increases and shows maxima at 318K and then decreases at 328K.. The adsorption of the inhibitor on the mild steel in 0.5M H_2SO_4 was found to obey Langmuir's adsorption isotherm. Scanning electronic microscopy (SEM) confirmed the existence of an adsorbed protective film on the metal surface. The kinetic and thermodynamic parameters were calculated and discussed.
Key Words: CMC, Corrosion Inhibition, EIS, Mild steel, Surfactant

I. Introduction

Mild steel is widely used as a constructional material in many industries due to its excellent mechanical properties and low cost. Mild steel being a material of choice in various industries undergo severe corrosion during acid cleaning, pickling, descaling etc. But its susceptibility to rusting in humid air and high dissolution rate in acidic medium are the major obstacles in its use on a large scale. The use of inhibitors is one of the most practical methods for protection against corrosion in acidic medium. The addition of surfactants to acidic media is an efficient and quite cheap method for corrosion inhibition of metal surfaces. Surfactants were used for electroplating venture because of the various beneficial effects. Surfactants have many advantages, for example, high inhibition efficiency, low price, low toxicity and easy production. An increase in inhibitory action was observed when the concentration of the surfactant in the corrosive solution approaches the critical micelle concentration (CMC). Above this value, there was no further increase in the efficiency that remains constant for further increase in surfactant concentration. In the absence of a charged head group, the driving force of micellization is the hydrophobic force and van der Waals attractions. However, very little work has yet been reported on cationic surfactants as inhibitors for mild steel corrosion in acidic medium. Bereket et al [1] investigated the inhibition of corrosion on low carbon steel using quaternary ammonium compounds and surfactant, cetyl trimethyl ammonium bromide. El Maghraby et al [2] studied the inhibitor behavior of cetyl trimethyl ammonium bromide for mild steel corrosion in 1M HCl and 2M HCl. Vasudevan et al [3] studied the influence of n- Hexadecyl pyridinium chloride on the corrosion of mild steel in 5N HCl and 5N H_2SO_4 .

The present study aimed to investigate the efficiency of new surfactant DPDAB as a corrosion inhibitor for mild steel in acidic medium. An attempt was also made to clarify the effects of concentration and temperature on the inhibition efficiency (%I) of studied inhibitor.

II. Experimental

2.1 Chemicals and materials

Hydrochloric acid (37 %), ethyl alcohol and acetone were purchased from SLR chemical company. N,N-Dimethyl-N-(2-Phenoxyethyl)dodecan-1- aminiumbromide(DPDAB) was purchased from sigma Aldrich Chemical Company. Bidistilled water was used for preparing test solutions for all measurements .The corrosion tests were performed on carbon steel with composition (weight %): C: 0.223, Mn: 0.505, P: 0.077, Si: 0.164 and Fe: 98.7.

2.2 Methods
2.2.1 Weight loss measurement

The specimen were cut into rectangular shape with an exposed area of 2cm x 1cm and were mechanically polished with various grades of emery paper(0/0, 2/0, 4/0 and 6/0) and then cleaned with ethanol and acetone followed by cleaning with double distilled water and finally dried. The specimens were weighed by using electronic digital balance (Uni Bloc AUY220 series) and finally suspended in a beaker containing 100ml of acid solution with and without inhibitor. The beakers were kept in a thermostat. After the specified time of immersion (3h), the specimens were removed, washed in distilled water, dried, placed in desiccators to attain room temperature and weighed. The experiments were carried out in triplicate.

The corrosion rate was calculated by the relation (1):

$$\text{corrosion rate} \left(\frac{mm}{y}\right) = \frac{87.6W}{DAT} \tag{1}$$

Where W = weight loss in mg, D = Density (g/cm^3), A = area in square centimeter, T= time in hour.

The percentage inhibition efficiency is calculated using the relation (2):

$$IE(\%) = \frac{w_0 - w_i}{w_0} \text{ x } 100 \tag{2}$$

Where w_i and w_0 are the weight loss values in the presence and in the absence of inhibitor respectively.

2.2.2 Electrochemical measurements

The electrochemical techniques used to study the corrosion behavior are potentiodynamic polarization and electrochemical impedance spectroscopy (EIS). The electrochemical experiments were carried out in a three electrode cell. Mild steel welded with copper wire and embedded in Teflon holder using epoxy resin with an exposed area 1cm^2 as working electrode, a platinum foil of 1cm^2 was used as counter electrode and the reference electrode was a saturated calomel electrode (SCE) with a luggin capillary, which can be at close proximity to the working electrode to minimize ohmic drop. All potentials are measured with respect to SCE.

The polarization and EIS studies were carried out using CHI Electrochemical workstation model 660C series. The potentiodynamic curves were obtained by scanning the potential range from cathodic potential of -200 mV to an anodic potential of + 200 mV vs SCE with respect to the open circuit potential at a scan rate of 10 mV/S. Equillibrium time leading to the steady state of specimen was 1h and the open circuit potential was noted. The experiments were carried out in triplicate.

The percentage corrosion inhibition efficiency was calculated from the relation (3):

$$\%IE = \frac{i_{corr}^0 - i_{corr}}{i_{corr}^0} \text{ x } 100 \tag{3}$$

Where i_{corr}^0 and i_{corr} are the corrosion current densities in absence and presence of various concentrations of the inhibitor.

The electrochemical impedance measurements were performed at corrosion potential over a frequency range 100 KHz to 0.01Hz with signal amplitude of 10 mV. The impedance data were analyzed and fitted using Zsimpwin software.

The percentage corrosion inhibition efficiency was calculated using the relation (4):

$$\%IE = \frac{R_{ct} - R_{ct}^0}{R_{ct}} \text{ x } 100 \tag{4}$$

Where R_{ct} and R_{ct}^0 are the charge transfer resistance of mild steel with and without inhibitor.

III. Results And Discussion

3.1 Weight loss measurements

The values of IE and corrosion rate obtained from weight loss measurements for MS in 0.5M H$_2$SO$_4$ containing different concentrations of DPDAB at different temperatures viz. 298 K, 308K, 318K and 328 K are tabulated in the Table 1. The variation of % IE with concentrations is depicted in Fig. 1. From the Fig.1. it is clear that the IE increases with increase of concentration reaching a maximum value at a higher concentration (10^{-2}M). This suggests that increase in the inhibitor concentration increases the number of molecules adsorbed over the mild steel surface, blocking the active sites by acid attack thereby protecting the metal surface from corrosion. The % IE decreases with increase in temperature from 298 – 308K again increase from 308 – 318 K and then decreases at 328 K as shown in the Fig. 2.

3.2 Potentidynamic (Tafel) polarization measurement

The cathodic and anodic polarization measurements for mild steel in stirred 0.5M H$_2$SO$_4$ containing different concentrations of DPDAB and at different temperatures (298 K – 328K) were carried out and Tafel plots were constructed. Fig. 3 shows the Tafel plots for mild steel in the absence and presence of different

concentration of DPDAB and at different temperatures in stirred 0.5M H_2SO_4 solution. From the Fig. 3. It is clearly seen that DPDAB shifted both the anodic and cathodic polarization curves to lower values of current density indicating the inhibition of both hydrogen evolution and mild steel dissolution reactions. Further the shift in the E_{corr} values is < 85mV suggest that the studied inhibitors act as mixed type inhibitor with predominantly of anodic type.

The polarization parameters are given in the Table 2. From the Table 2 it is clear that the the values of corrosion current density decreased significantly with increase in the concentration of DPDAB. Corrosion potential values shifted towards more noble direction with increase in the concentration of DPDAB. The percentage inhibition efficiency increased with increase in the concentration of inhibitors from 96.7% to 99.1% for DPDAB.The inhibition effect of the surfactants mainly depends upon the critical micelle concentration (CMC). CMC is a key factor in determining the effectiveness of surfactants as corrosion inhibitors. According to Free [4], CMC can be determined by plotting $1/i_{corr}$ against surfactant concentration. From the Fig.4 the value of CMC for DPDAB is found to be approximately 10^{-3}M. From the Fig. 1 it is evident that above the CMC, increasing surfactant concentration leads to the gradual formation of multilayers that further reduces the rate of corrosion thereby increasing the percentage corrosion inhibition efficiency .

However, concentration changes above CMC lead to smaller changes in inhibition, since the changes above the CMC result only in additional coverage beyond the monolayer level, which is already sufficient for significant inhibition. This situation is analogous to adding a second coating of paint to protect a surface that is already protected by an initial coating. It is likely that additional surface coverage in the form of multilayer that results at surfactant concentrations above the CMC are responsible for the additional increase in corrosion inhibition above the CMC. The reason for this explanation is simple. At coverages of one monolayer or less, surfactant molecules can inhibit either the cathodic or anodic reaction by occupying reactive sites, or by simply providing resistance to the supply of oxidant or the transport of reaction products. Once the surface is filled with surfactant molecules and additional molecules form multiple layer structures, the added surfactant molecules no longer have direct access to the surface. Consequently, the additional molecules that adsorb at concentrations above the CMC must inhibit corrosion by offering additional resistance to the transport of necessary elements rather than by occupying reactive sites directly. The higher corrosion inhibition efficiency in DPDAB is attributed to the presence of both delocalized π- electrons and lone pair of electrons on nitrogen atom followed by the synergistic effect of Br⁻ ions.

From the Table 2 it is evident that the corrosion inhibition efficiency decreases from increasing the temperature from 298 K – 308 K and then increases and shows maxima at 318K and then decreases at 328 K [Fig. 2] this is indicative of the fact that the DPDAB undergoes change in orientation of phenyl ring as the temperature increases. At 318 K, they may be in the same plane, therefore enhancing the adsorption on the metal surface. This change in orientation of phenyl ring is not possible beyond a certain temperature because of the shorter time lag between adsorption – desorption processes [5]. From the Table 2 it is clear that DPDAB is a very efficient inhibitor at all studied temperature especially at higher concentrations.

3.3 Electrochemical impedance spectroscopy:

Electrochemical impedance measurements were conducted for mild steel in 0.5M H_2SO_4 as well as acid containing different concentration of inhibitors DPDAB at 25°C. The impedance data was analyzed using the circuit shown in the Fig. 5. The fitted data follows almost the same pattern as the experimental results with R(Q(R(QR)) equivalent circuit using the Zsimpwin software. Fig. 6 shows the Nyquist and Bode plots for mild steel in 0.5M H_2SO_4 and 0.5M H_2SO_4 containing different concentration of DPDAB. Table 3 gives the values of electrochemical impedance parameters obtained from the fitting procedure. The values of Y_a & Y_{dl} (Y_a & Y_{dl} can be regarded to be approximation to the values of the adsorption capacitance and double layer capacitance respectively) has decreasing trend for the adsorption of the inhibitors on the metal surface, suggesting the inhibitor molecules displace water molecules originally adsorbed on the metal surface. The R_{ct} value increases with increase in concentration thereby increasing the % IE with increase in concentration of the inhibitor. The C_{dl} related to Y_{dl} decreases with the increase in DPDAB concentration. The decrease in C_{dl} values may be due to the decrease in local dielectric constant and or increase in the thickness of the double layer. The Values of n_a associated with $(CPE)_a$ for the inhibitor was found to be 1 which indicates a near capacitive behavior of the surface film formed on the Mild steel sample. The values of n_{dl} related to $(CPE)_{dl}$ are found to be in the range 0.5 to 0.7 for DPDAB indicating the electrode surfaces are partially heterogeneous.

IV.   Adsorption Isotherms And Thermodynamic Parameters

Adsorption of surfactants on solid surfaces can modify their hydrophobicity, surface charge and other key properties that govern interfacial processes such as corrosion inhibition [6]. In general, adsorption is governed by a number of forces such as covalent bonding, electrostatic attraction, hydrogen bonding and non-polar interactions between the adsorbed species, lateral associative interaction, solvation and desolvation [7].

The total adsorption is usually the cumulative result of some or all of the above forces. Several adsorption isotherms were assessed and the Langmuir adsorption isotherm was found to be the best description of the adsorption behavior of the surfactant under investigation in the acidic medium. Fig. 7 shows a plot of C/θ against C. The slope of the straight line is nearly or equal to unity.

Thus it can be concluded that DPDAB adsorbed at the steel surface following Langmuir isotherm model without interaction between the adsorbed molecules. Table 4 lists the thermodynamic parameters for adsorption of DPDAB in 0.5M H_2SO_4 on the mild steel surface. The values of ΔG^o_{ads} for DPDAB on mild steel surface in 0.5M H_2SO_4 are highly negative. This suggests that the inhibitor interact strongly with the mild steel surface. Values of ΔG^o_{ads} were found to be around -33.0KJ/mol indicates that the adsorption mechanism involves two types of interaction, Physisorption and chemisorptions. From the values of free energy of adsorption (ΔG^o_{ads}) and enthalpy of adsorption (ΔH^o_{ads}), the entropy of adsorption (ΔS_{ads}) was calculated using Gibb's – Helmholtz equation. The enthalpy of adsorption was obtained from the plot of $\log \frac{\theta}{1-\theta}$ vs 1/T at different concentrations of inhibitor as shown in Fig.8. The average value of ΔH^o_{ads} is given in Table 4. ΔH^o_{ads} is negative which indicates the adsorption of inhibitor molecules on mild steel surface is an exothermic process. The positive sign of ΔS^o_{ads}, means that the process is accompanied by an increase in entropy, which is the driving force for the adsorption of inhibitor onto the mild steel surface [8].

V. Effect Of Inhibitors On The Activation Parameters Of Corrosion Process

In order to obtain more details on the corrosion process, activation kinetic parameters such as energy of activation (E_a), enthalpy of activation ($\Delta H^{\neq}$) and entropy of activation ($\Delta S^{\neq}$) are evaluated using Arrhenius equation and the Transition state equation[9]. Fig.9 shows Arrhenius plots for mild steel in 0.5M H_2SO_4 with different concentrations of DPDAB. The activation energies are estimated from the slopes ($-E_a$/R). The transition state plot of the corrosion Current density for mild steel in 0.5M H_2SO_4 with different concentrations of DPDAB is shown in Fig. 10, these permit the calculation of ($\Delta H^{\neq}$) and ($\Delta S^{\neq}$), from slopes ($-\Delta H^{\neq}$/2.303R) and intercepts [log R/Nh + $\Delta S^{\neq}$/2.303R] respectively. The activation parameters for surfactant are tabulated in the Table 5. The activation energies in the presence of different concentrations of surfactant in 0.5M H_2SO_4 is higher than that in the absence of inhibitors. The decrease of inhibition efficiencies with increasing temperature and the increase in E_a in the presence of the inhibitors indicates that the adsorption may be physical adsorption in 0.5M H_2SO_4. The positive sign of the enthalpies of activation reflect the endothermic nature of dissolution process of steel in acidic medium. Large and negative value of entropies of activation imply that the activated complex in the rate determining step represents an association rather than a dissociation step, means that a decrease in disordering takes place on going from reactants to the activated complex [10].

6. Scanning electron microscopic studies:

Fig.11a shows the surface morphology of the polished mild steel surface before immersion in 0.5M H_2SO_4. SEM photographs after specimen immersion in 0.5M H_2SO_4 for 3h in the absence and presence of an optimum concentration of DPDAB are shown in the Fig. 11 b & c. It could be seen from the Fig. 11b that the specimen surface is strongly damaged and faceting seen as a result of pits formed due to the exposure of mild steel to the acid in the absence of the inhibitor. From the Fig. 11c it could be seen that in the presence of inhibitor, the faceting disappeared and the surface was free from pits and it was smooth. This reveals that there is a good protective film adsorbed on specimen surface, which was responsible for inhibition of corrosion.

VI. Mechanism

Mechanism of corrosion inhibition is complex and depends on the formation of mono- or multi-dimensional protective layers on the metal surface. The protective nature of the surface layers depends on the factors: interaction between inhibitors and substrate, incorporation of the inhibitor in the surface layer, chemical reactions, electrode potentials, concentration of the inhibitors, temperature and properties of the corresponding surface, etc. The first stage in the mechanism of the surfactants as corrosion inhibitors in aggressive media is adsorption of the surfactant molecules onto the metal surface. The adsorption process is influenced by the nature and the surface charge of the metal, the chemical structure of the surfactant, and the nature of the aggressive electrolyte. Adsorption of the surfactant molecules occurs because the interaction energy between the surfactant molecules and the metal surface is higher than that between water molecules and the metal surface. So the inhibition effect by surfactants is attributed to the adsorption of the surfactant molecules via their functional groups onto the metal surface. The adsorption rate is usually very rapid and hence the reactive metal is shielded from the aggressive environment. Corrosion inhibition depends on the adsorption ability of the surfactant molecules on the corroding surface, which is directly related to the capacity of the surfactant to aggregate to form micelles. The critical micelle concentration (CMC) is a key factor in determining the effectiveness of a corrosion inhibitor. Below CMC, the molecules tend to aggregate at the interface, and this interfacial aggregation reduces the surface tension. Above CMC the metal surface is covered with multilayers. This, consequently, does not alter the corrosion rate.

Banerijee and Mallhotra [11] reported the PZC for mild steel is -550mV in H_2SO_4, therefore $\emptyset_c$ is positive (+47.2) so the metal surface acquires slight positive charge in the acidic medium. Studied surfactant may chemisorb at steel / solution interface via chemical bond between positively charged nitrogen atoms and negatively charged mild steel surface as follows: Steel surface is positively charged in presence of H_2SO_4 medium. While bromide ion is negatively charged, as a result the specific adsorption of bromide ion occurs onto mild steel surface, causing negatively charged surface of steel. By means of electrostatic attraction, surfactant cation easily reaches mild steel surface, so bromide ion acts as an adsorption mediator for bonding metal surface and inhibitors. This gives rise to the formation of an adsorbed composite film in which Br^- ions are sandwiched between metal and positively charged part of inhibitor. This film acts as a barrier facing corrosion process.

VII. Conclusion

➢ Surfactants are proved to be one of the best eco-friendly anti-corrosion substances to protect the materials from corrosion. The high affinity of surfactant molecules to adsorb onto interfaces to form micelles is responsible for their applications in several interfacial systems making them very attractive to be used as corrosion inhibitors for metallic surfaces.

➢ Anti corrosion property of different types of surfactants can be potentially used in the industry as good option to solve the problems of corrosion of metallic surfaces to prevent the material and economic loss.

➢ Potentiodynamic polarization curves reveal that the inhibitor act as mixed type inhibitor.

➢ Electrochemical impedance spectroscopy results showed that the corrosion inhibition of mild steel occurs mainly by charge transfer.

➢ Generally, values of ΔG^o_{ads} around -20kJ/mol or lower are consistent with the electrostatic interaction between charged molecules and the charged metal surface (Physisorption); those around -40kJ/mol or higher involve charge sharing or transfer from organic molecules to the metal surface to form a coordinate type of metal bond (Chemisorption). In the present work, the calculated ΔG^0_{ads}, values are slightly less negative than -40 kJ/mol indicating that the adsorption of inhibitor molecules is not merely physisorption or chemisorption but obeying a comprehensive adsorption(Physical and chemical adsorption).

➢ The E_a values in 0.5M H_2SO_4 containing inhibitors were higher than that for the uninhibited one, indicating a strong inhibitive action for the studied compounds by increasing the energy barrier for the corrosion process, thus emphasizing the electrostatic character of the inhibitor's adsorption on mild steel surface.

➢ The ΔH^o_{ads} values are negative for all the studied inhibitors in 0.5M H_2SO_4, suggests that the adsorption of inhibitor molecules onto metal surface is an exothermic process.

Acknowledgement

References

[1]. Bereket G. and A. Yurt, Inhibition of the corrosion of low carbon steel in acidic solution by selected quaternary ammonium compounds, Anti-Corrosion Methods and Materials, 49(3), 2002, 210-220.

[2]. El Maghraby A.A. and T.Y. Soor, Efficient cationic surfactant as corrosion inhibitor for carbon steel in Hydrochloric acid solutions, Pelagia Research Library, Advances in Applied Science Research, 1(2), 2010, 156-168.

[3]. Vasudevan T., B. Muralidharan, S. Muralidharan and S. Venkatakrishna Iyer, Inhibition of corrosion of mild steel in acidic solutions by Quaternary salts of Pyridinium bases, Anti-Corrosion Methods and Materials, 45(2),1998, 120-126.

[4]. Free M.L., Understanding the effect of surfactant aggregation on corrosion inhibition of mild steel in acidic medium, Corros. Sci., 44, 2002, 2865.

[5]. Kalpana Bhrara, Gurmeet Singh and Hansung Kim, Inhibiting effects of butyl triphenyl phosphonium bromide on corrosion of mild steel in 0.5 M sulphuric acid solution and its adsorption characteristics, corros. Sci., 50,2008, 2747-2754.

[6]. Grieves R.B and Somasundaran P, Advances in interfacial phenomena of particulate/solution/gas systems, AICHE symposium series, 71,1975, 124.

[7]. Fuertenau D.W. The adsorption of surfactants at solid/water interfaces in : Hair ML, editor. The chemistry of biosurafces, (New York. 1971) 143.

[8]. Li X.H., F.Z. Yang, G.N. Mu, H.Fu and S.D. Deng, Inhibition effect of nonionic surfactant on the corrosion of cold rolled steel in HCl, Corros. Sci., 50, 2008, 420-430.

[9]. Prathibha B.S, P. Kotteeswaran, V. Bheema raju, Study on the inhibition of Mild steel corrosion by N, N- dimethyl-N-(2-phenoxyethyl) dodecan-1-aminiumbromide in HCl Medium, IOSR-JAC, 2(5), 2012, 61-70.

[10]. Bentiss F., M. Lebrini and M. Lagrenee, Thermodynamic characterization of metal dissolution and inhibitor adsorption processes in mild steel/2,5-bis(n-thienyl)-1,3,4-thiadiazoles/hydrochloric acid system, Corros. Sci., 47,2005, 2915-2931.

[11]. Banerijee G. and S.N. Malhotra, Contribution to adsorption of aromatic amines on mild steel surface from HCl solutions by impedance, UV and Raman spectroscopy, Corrosion, 48,1992, 10-15.
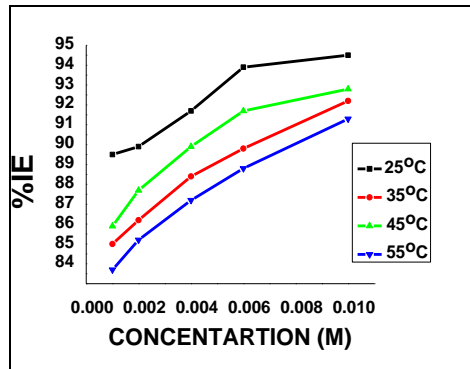
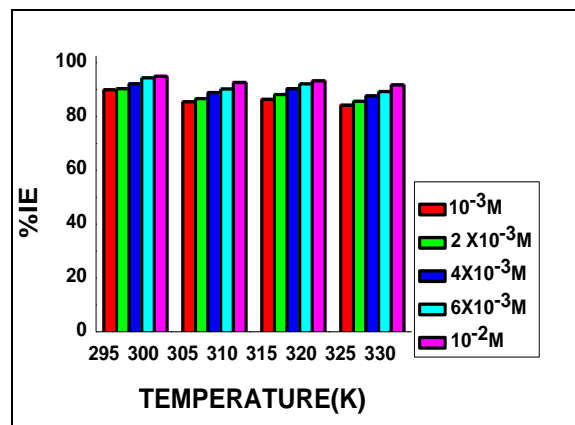**Figure 1.** Variation of %IE with concentration of the studied Inhibitor

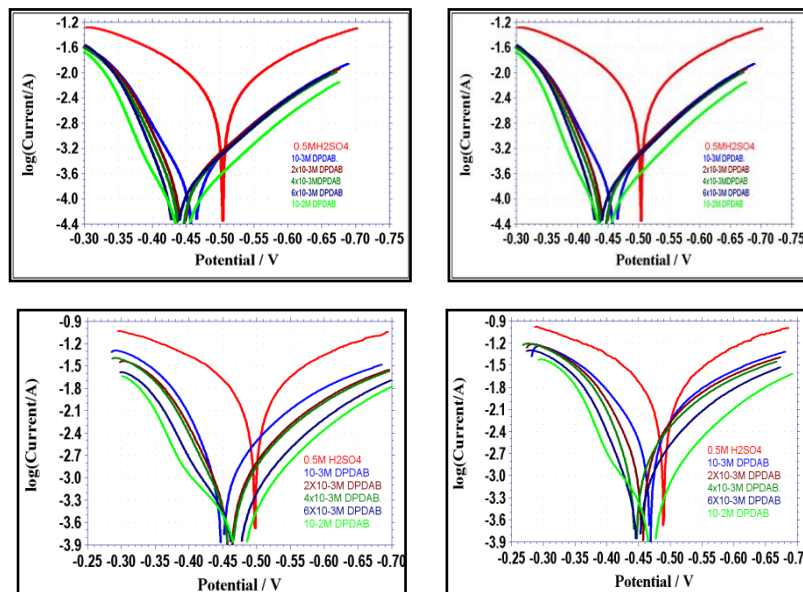**Figure 2.** Variation of %IE with temperature for different concentrations

Figure 3. Tafel plots for mild steel in 0.5M H_2SO_4 in the absence and presence of different concentrations of DPDAB at 1) 298 K 2)308K 3) 318K and 4) 328K
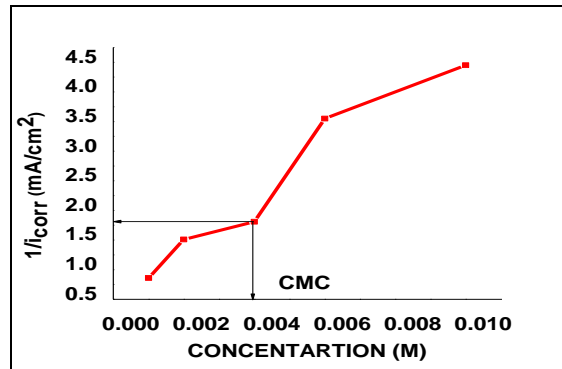
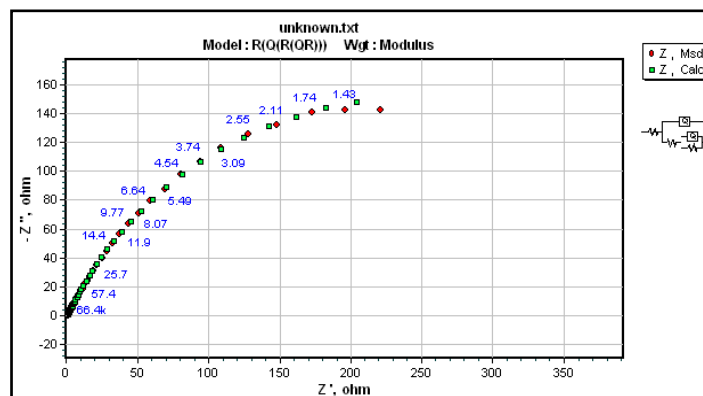**Figure 4 .** Variation of $1/i_{corr}$ against concentration

Figure 5. Equivalent circuit model used to fit the impedance data for DPDAB in 0.5M H_2SO_4
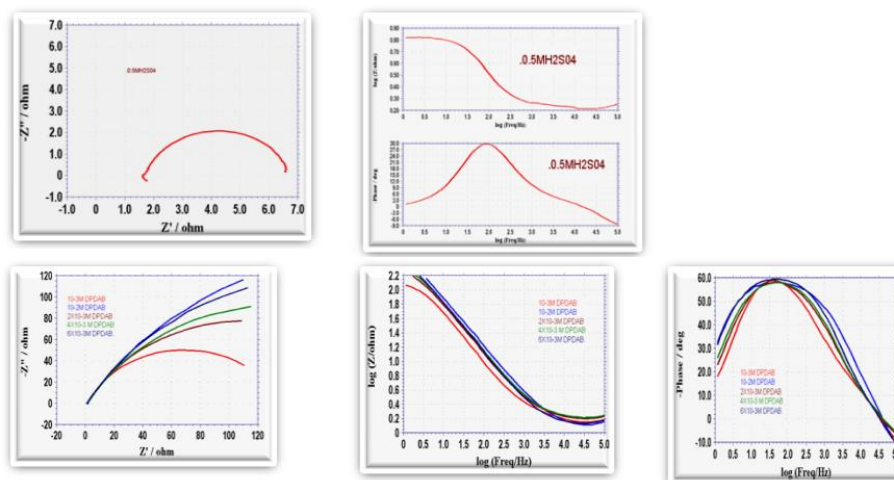

Figure 6. Nyquist and Bode plots for mild steel in 0.5M H_2SO_4 containing different concentrations of DPDAB at 25^oC
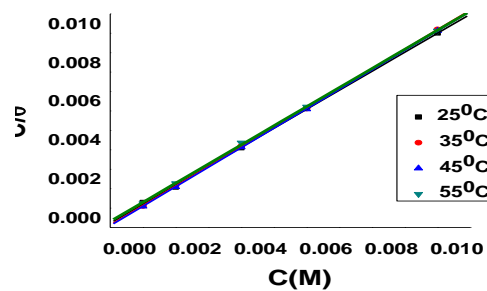
Figure 7 Plot of Langmuir adsorption isotherm for mild steel in 0.5M H_2SO_4 containing DPDAB
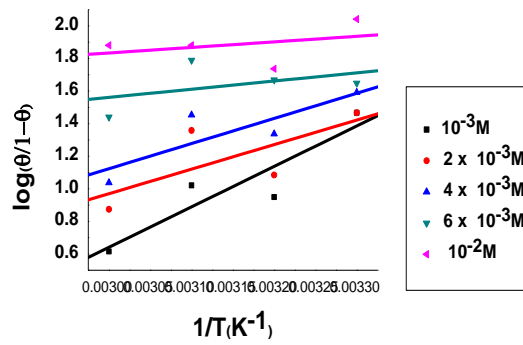
Figure 8 Plot of log(θ/1- θ) vs 1/T for mild steel in 0.5M H$_2$SO$_4$ + DPDAB
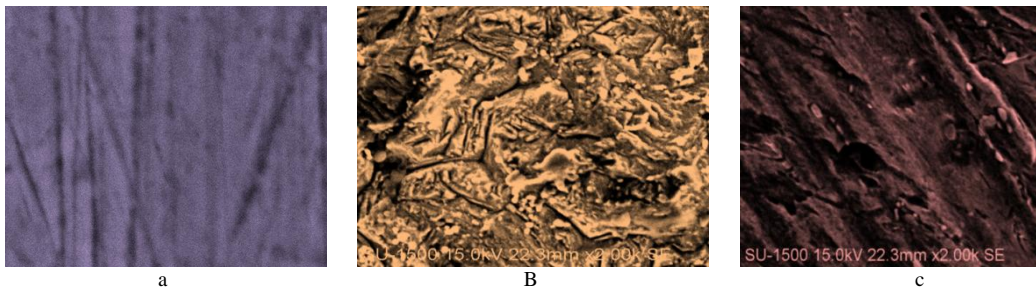
Figure 9. Arrhenius plot for Mild steel in 0.5M H$_2$SO$_4$ without and with different concentration of DPDAB
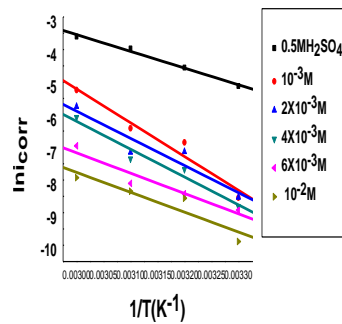
Figure 10. Transition state plot for Mild steel in 0.5M H$_2$SO$_4$ without and with different concentration of DPDAB

Figure 11. Surface Characterization by SEM for a) Polished mild steel b) In 0.5M H$_2$SO$_4$ c) 0.5M H$_2$SO$_4$ + DPDAB

Table 1

Inhibition efficiency of DPDAB with different concentration and temperature for the corrosion of mild steel in 0.5M H_2SO_4 by weight loss method (298K-328K).

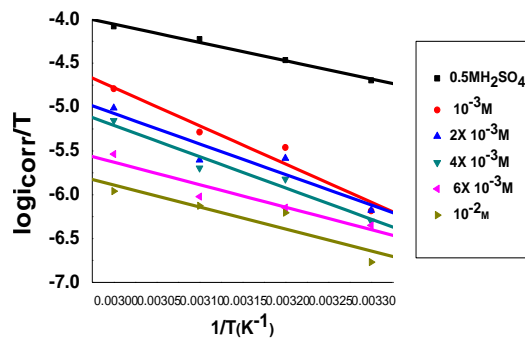| Inhibitor concentration (M)	%IE	Corrosion rate(mm/y)	308K		318K		328K	
			%IE	Corrosion rate(mm/y)	%IE	Corrosion rate(mm/y)	%IE	Corrosion rate(mm/y)
Blank		59.88		112.89		225.8		410.1
1×10^{-3}	90.0	5.95	85.5	16.37	86.4	30.68	84.2	64.72
2×10^{-3}	90.4	5.76	86.7	15.06	88.2	26.59	85.7	58.58
4×10^{-3}	92.2	4.65	88.9	12.46	90.4	21.57	87.7	50.40
6×10^{-3}	94.4	2.35	90.3	10.97	92.2	17.67	89.3	43.89
1×10^{-2}	95.0	2.97	92.7	8.18	93.3	15.06	91.8	33.66

Table 2

Electrochemical polarization parameters for Mild Steel in 0.5M H_2SO_4 containing different concentrations of DPDAB at different temperatures

Concentration (M)	E_{corr} (mV)	i_{corr} ($\mu A/cm^2$)	b_a (mV/decade)	b_c (mV/decade)	%IE
298 K					
Blank	-495.4	18910	201.9	203.9	
1×10^{-3}	-485.8	1644	132.2	109.5	91.3
2×10^{-3}	-497.5	790.6	125.2	82.1	95.8
4×10^{-3}	-497.3	641.2	123.6	74.9	96.6
6×10^{-3}	-499.1	302.9	115.4	60.0	98.4
1×10^{-2}	-501.1	237.4	112.9	64.7	98.7
6×10^{-3}	-476.4	219.4	66.6	109.7	97.9
1×10^{-2}	-492.0	191.9	83.7	109.9	98.2
318K					
Blank	-495.4	18910	203.8	201.9	
1×10^{-3}	-485.8	1644	109.5	132.2	91.3
2×10^{-3}	-497.5	790.6	82.1	125.2	95.8
4×10^{-3}	-497.3	641.2	74.9	123.6	96.6
6×10^{-3}	-499.1	302.9	60.0	115.4	98.4
1×10^{-2}	-501.1	237.4	64.7	112.9	98.7
328K					
Blank	-485.9	27230	196.2	201.1	
1×10^{-3}	-481.6	5296	124.7	178.6	80.5
2×10^{-3}	-474.5	3197	115.9	158.9	88.2
4×10^{-3}	-467.6	2292	118.5	140.2	91.6
6×10^{-3}	-473.9	954.4	87.4	125.2	96.5
1×10^{-2}	-493.5	360.5	52.8	117.5	98.7

Table 3

Impedance parameters for mild steel in 0.5M H_2SO_4, absence and presence of different concentration of DPDAB at 25°C

Concentration (M)	Y_a ($\Omega^{-1} cm^{-2} S^{n_{dl}} 10^{-4}$)	n_a	R_a (Ω)	C_a ($\mu F/cm^2$)	Y_{dl} ($\Omega^{-1} cm^{-2} S^{n_{dl}} 10^{-4}$)	n_{dl}	R_{ct} (Ω)	C_{dl} ($\mu F/cm^2$)	(%)IE
Blank					15.39	0.8657	5.016	723.6	
1×10^{-3}	0.5027	1	1.74	50.27	6.585	0.7887	138.1	346.4	96.4
2×10^{-3}	0.4956	1	2.676	49.56	6.48	0.6911	233.4	303.5	97.8
4×10^{-3}	0.4522	1	2.724	45.22	6.444	0.6629	291.1	275.1	98.3
6×10^{-3}	0.4213	1	3.231	42.13	6.364	0.5755	382.3	224.3	98.7
1×10^{-2}	0.3260	1	3.742	32.6	6.186	0.5335	492.6	218.8	98.9

Table 4

Thermodynamic parameters obtained from adsorption isotherms for DPDAB in 0.5M H_2SO_4

Temperature (K)	R	Slope	K_{ads}	ΔG^o_{ads} (kJ/mol)	ΔH^o_{ads} (kJ/mol)	ΔS^o_{ads} (J/mol/K)
298	0.9977	0.9977	12780.8	-33.4	-24.4	30.2
308	0.9999	1.0066	7982.6	-33.3	-24.4	28.8
318	0.9999	1.0053	10954.2	-35.2	-24.4	33.9
328	0.9998	0.9848	3165.6	-32.9	-24.4	25.9

Table 5

Corrosion kinetic parameters for mild steel in 0.5M H_2SO_4, absence and presence of different concentrations of DPDAB

Concentration (M)	E_a (kJ/mol)	$\Delta H^{\neq}$ (kJ/mol)	$\Delta S^{\neq}$ (J/mol/K)
Blank	42.6	39.9	-155.3
1 X 10^{-3}	50.6	47.9	-38.9
2 X 10^{-3}	51.7	49.1	-92.4
4 X 10^{-3}	69.2	66.3	-94.8
6 X 10^{-3}	70.9	68.3	-158.0
1 X 10^{-2}	86.0	83.4	-166.3